International Journal of Mechanical, Industrial and Aerospace Sciences
ISSN: 2517-9950
Vol:3, No:10, 2009

Sensorless Control of a Six-Phase Induction Motors Drive Using FOC in Stator Flux Reference Frame

G. R. Arab Markadeh, J. Soltani, N. R. Abjadi, M. Hajian

Abstract**—**In this paper, a direct torque control - space vector modulation (DTC-SVM) scheme is presented for a six-phase speed and voltage sensorless induction motor (IM) drive. The decoupled torque and stator flux control is achieved based on IM stator flux field orientation. The rotor speed is detected by on-line estimating of the rotor angular slip speed and stator vector flux speed. In addition, a simple method is introduced to estimate the stator resistance. Moreover in this control scheme the voltage sensors are eliminated and actual motor phase voltages are approximated by using PWM inverter switching times and the dc link voltage. Finally, some simulation and experimental results are presented to verify the effectiveness and capability of the proposed control scheme.

Keywords**—**Stator FOC, Multiphase motors, sensorless.

I. Introduction

IN recent past, multiphase motor drives have been proposed by several authors [1-5]. Many different solutions have been suggested to exploit different advantages, such as [6]:

1) To decrease the single switches current stress instead of adopting parallel techniques.
2) To smooth the electromagnetic torque pulsations.
3) To reduce the harmonics content of the DC link current.
4) To improve the overall system reliability.

Among the different multiphase drive solutions, one of the most interesting and extensively discussed in the literature is the dual three-phase IM having two sets of three-phase windings spatially shifted by 30 electrical degrees (so called quasi-six-phase machine). Neutral points of the two windings can be isolated or connected.

The major reason for selecting the asymmetrical six-phase winding instead of the true six-phase winding (60^o displacement between any two consecutive phases), elimination of the sixth harmonic from the torque [3], was important in the pre-pulse width-modulation (PWM) era of VSI control. A quasi six-phase IM is used in the work described here, with the underlying idea of realizing a motor drive system with a simple control, while utilizing a single six-phase SVPWM VSI as the supply.

The customary method to speed/torque control of an IM is rotor flux field-oriented control (FOC). Using FOC, one observes that, by holding the magnitude of the flux constant, there is a linear relationship between a control variable and the torque

One may note that the rotor flux orientation scheme is very sensitive to IM parameters variations and uncertainties especially IM rotor resistance and machine magnetization inductance [7].

The DTC-SVM is based on stator FOC and used for independent control of IM torque and stator flux

Speed sensorless control methods of IM drives are common either because a speed sensor cannot be installed for safety or environmental reasons or for reducing both the cost and the size of the whole drive. Therefore, many studies are still being devoted to the removal of the speed sensor, while maintaining the performance of the system [8]-[14].

In this paper, a simple speed estimator is proposed which is applicable for wide range of rotor speed estimation. In addition, a stator resistance estimator is also introduced for on-line detecting of this parameter.

The proposed control scheme is verified by both the simulation and experimental results.

II. Description and Modeling of the Drive System

The motor drive system is supplied from a two level SVPWM VSI. Each machine has its own set of parameters. Based on Clarke's transformation described by the following matrix C, the $(\alpha-\beta)$, $(x-y)$ and (zero sequence) equivalent circuits of each motor in the stationary reference frame are obtained.

$$C=\sqrt{\frac{2}{6}}\begin{array}{r}\alpha\\ \beta\\ x\\ y\\ 0+\\ 0-\end{array}\begin{bmatrix}1 & \cos\phi & \cos 4\phi & \cos 5\phi & \cos 8\phi & \cos 9\phi\\ 0 & \sin\phi & \sin 4\phi & \sin 5\phi & \sin 8\phi & \sin 9\phi\\ 1 & \cos 5\phi & \cos 8\phi & \cos\phi & \cos 4\phi & \cos 9\phi\\ 0 & \sin 5\phi & \sin 8\phi & \sin\phi & \sin 4\phi & \sin 9\phi\\ 1 & 0 & 1 & 0 & 1 & 0\\ 0 & 1 & 0 & 1 & 0 & 1\end{bmatrix} \quad (1)$$

where $\phi=\pi/6$ [4].

G. R. Arab Markadeh., is with Department of Engineering, Shahrekord University, Shahrekord, Iran (e-mail: arab-gh@eng.sku.ac.ir).

J. Soltani is with the Department of Engineering, Islamic Azad University – Khomeinishahr Branch, Khomeinishahr, Isfahan, Iran (+98-311-4416176; fax: +98-311-391-2451; e-mail: j1234sm@c.iut.ac.ir).

N. R. Abjadi and M. Hajian are with the Department of Electrical and Computer Engineering, Isfahan University of Technology, Isfahan, Iran (+98-913-2686959; fax: +98-311-391-2451; e-mail: navidabjadi@yahoo.com).

The stator and rotor voltage equations for each machine are given as

$$\begin{cases} v_{ks} = R_s i_{ks} + \frac{d}{dt}(L_s i_{ks} + L_m i_{kr}) \text{ for } k = \alpha, \beta \\ v_{ks} = R_s i_{ks} + \frac{d}{dt}(L_{ls} i_{ks}) \text{ for } k = x, y \end{cases} \quad (2)$$

$$\begin{cases} 0 = R_r i_{\alpha r} + \omega_r (L_r i_{\beta r} + L_m i_{\beta s}) + \\ \quad \frac{d}{dt}(L_r i_{\alpha r} + L_m i_{\alpha s}) \\ 0 = R_r i_{\beta r} - \omega_r (L_r i_{\alpha r} + L_m i_{\alpha s}) + \\ \quad \frac{d}{dt}(L_r i_{\beta r} + L_m i_{\beta s}) \end{cases} \quad (3)$$

The torque equations of the machine is given by

$$T_e = P\ L_m (i_{\alpha r} i_{\beta s} - i_{\beta r} i_{\alpha s}) \quad (4)$$

where P is the number of pole pairs. One may note that the torque production currents are $(i_{\alpha s}, i_{\beta s})$ and (i_{xs}, i_{ys}) are non-producing torque currents.

III. IM Stator FOC

Fig. 1 shows the control block diagram of a direct torque controlled IM drive in the stator flux field oriented reference frame (FOC) corresponding to this machine. The control loop consists of three PI controllers, and the SVPWM is used for maximum utilization of dc link voltage and easy digital implementation.

The angle of stator flux vector is given by

$$\theta_e = \arctan \frac{\lambda_{\beta s}}{\lambda_{\alpha s}} \quad (5)$$

Differentiating from (5) one can obtain the angular speed of stator flux vector as

$$\omega_e = \frac{\dot{\lambda}_{\beta s} \lambda_{\alpha s} - \dot{\lambda}_{\alpha s} \lambda_{\beta s}}{\lambda_s^2} \quad (6)$$

Substituting for derivative of stator flux components in (6), the synchronous speed is written as

$$\omega_e = \frac{(v_{\beta s} - R_s i_{\beta s}) \lambda_{\alpha s} - (v_{\alpha s} - R_s i_{\alpha s}) \lambda_{\beta s}}{\lambda_s^2} \quad (7)$$

The phase voltages needed in these equations are obtained as follow.

First the phase to negative point of dc link (N) voltages are obtained

$$v_{jN} = \frac{v_{DC} t_j}{T_s} \quad (8)$$

where $j = a, b, c, d, e, f$.

then the phase voltages are given as

$$v_{js} = \frac{1}{6}(5 v_{jN} - \sum_{i=a,\, i \neq j}^{f} v_{iN}) \quad (9)$$

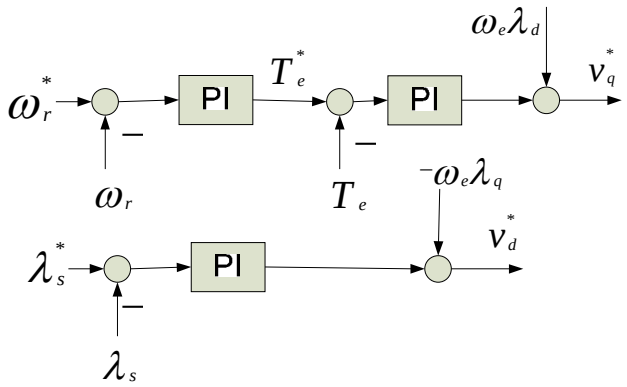

Fig. 1 FOC block diagram

Assuming the stator currents are measured and stator flux components are obtained from the following flux observer.

Flux observer:

$$\begin{cases} \lambda_{\alpha s} = \int (v_{\alpha s} - R_s i_{\alpha s}) dt \\ \lambda_{\beta s} = \int (v_{\beta s} - R_s i_{\beta s}) dt \end{cases} \quad (10)$$

IV. Rotor Speed Estimator

The IM rotor flux linkages in a two axis stationary reference frame are obtained as

$$\begin{cases} \lambda_{\alpha r} = \frac{L_r}{L_m}(\lambda_{\alpha s} - L_s i_{\alpha s}) + L_m i_{\alpha s} \\ \lambda_{\beta r} = \frac{L_r}{L_m}(\lambda_{\beta s} - L_s i_{\beta s}) + L_m i_{\beta s} \end{cases} \quad (11)$$

$$\lambda_r = \sqrt{\lambda_{\alpha r}^2 + \lambda_{\beta r}^2} \quad (12)$$

Considering the IM rotor flux field orientation reference frame [15]

$$\begin{cases} \lambda_{dr}^r = L_m i_{ds}^r = \lambda_r \\ \frac{L_m}{T_r} i_{qs}^r = \omega_{sl} \lambda_{dr}^r = \omega_{sl} \lambda_r \end{cases} \quad (13)$$

The IM electromagnetic generated torque is obtained as

$$T_e = P\ \frac{L_m}{L_r}(\lambda_{\alpha r} i_{\beta s} - \lambda_{\beta r} i_{\alpha s}) = P\ \frac{L_m}{L_r} \lambda_{dr}^r i_{qs}^r \quad (14)$$

Combining (13) and (14) gives

$$\omega_{sl} = \frac{R_r T_e}{P\ \lambda_r^2} \quad (15)$$

The rotor speeds can be detected from the following equation

$$\hat{\omega}_r = \hat{\omega}_e - \omega_{sl} \quad (16)$$

where $\hat{\omega}_e$ is the rotor synchronous speed which in fact is the on-line speed of the rotor vector flux (λ_r); in other words

$$\hat{\omega}_e = \frac{d}{dt} \arctan \frac{\lambda_{\beta s}}{\lambda_{\alpha s}} \quad (17)$$

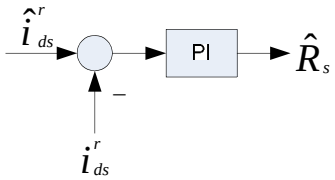

Fig. 2 Estimation of IM stator resistance

V. Stator Resistance Estimator

Using (13), yields

$$\hat{i}_{ds}^{r} = \frac{\lambda_r}{L_m} \tag{18}$$

Transferring $i_{\alpha s}$ from stationary reference frame (α, β) to rotor flux field orientation reference frame (d^r, q^r), the stator resistance can be detected by using a conventional PI regulator as shown in Fig. 2.

VI. Experimental Results

Simulation and Experimental results are obtained for a six-phase squirrel cage IM with parameters shown in Table I. The overall system block diagram is shown in Fig. 3.

The experimental rig is illustrated in Fig. 4. A dual-three phase IM drive have been constructed to perform the experimental tests. The switching frequency of the six-phase IGBT inverter has been set at 4 kHz. The control software has been implemented on a PC. A Xilinx XC95288 CPLD is used for real time implementation of switching patterns and to send the data from some A/Ds used to measure currents and dc link voltage. The CPLD board communicates with PC via a digital Advantech PCI-1751 I/O board. A second Xilinx XC95108 CPLD is used to calculate and send the speed data from an encoder to computer through printer port. The currents are measured using LEM sensors. The control code is written in C. It performs closed loop speed control and rotor flux control. The quasi six-phase IM is obtained by rewinding the stator of a three-phase machines. A SVPWM strategy is used.

Simulation and experimental results are shown in Figs. 5-7 and Figs. 8-10 respectively.

In Figs. 5.a-5.c the results of speed start-up test are shown. The corresponding speed reference is linearly increased from zero to 100 rad/s in 2 seconds. The speed of the IM tends to its reference command in the proposed sensorless scheme. The stator flux magnitude achieves to its reference with a fast dynamics. The components of stator flux are sinusoidal and in quadrature to each other.

TABLE I. IM Parameters

Poles	2	R_s	9 Ω
R_r	8.37 Ω	L_s	740 mH
L_r	740 mH	L_m	712 mH
P_n	1 Kw	f_n	50 Hz

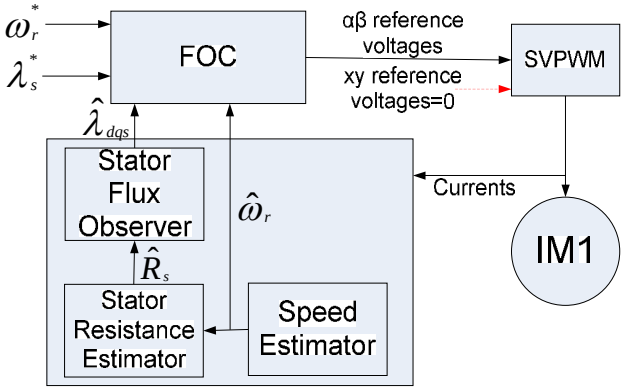

Fig. 3. Drive system block diagram.

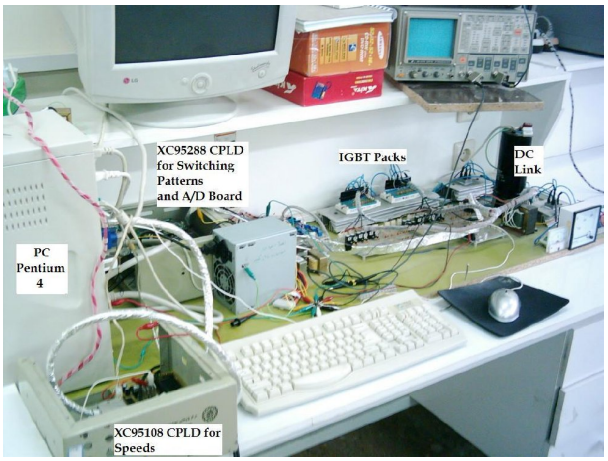

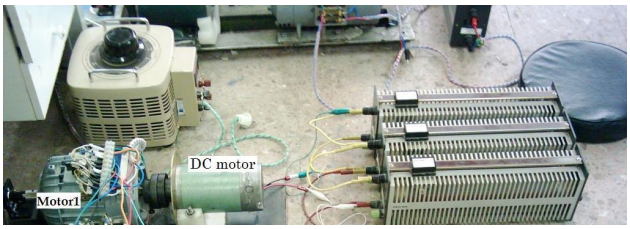

Fig. 4 Experimental rig: PC, CPLD boards and inverter (top), the six-phase IMs (bottom).

Figs. 6.a-6.c show the simulation results for the speed control (speed reversal) test. In this test the IM runs with positive speed (50 rad/s), then the speed of the IM is reversed linearly in 1 second for $t \in [5,6]$. The amplitudes of stator flux is kept constant on 0.9 Wb. These results verify the ability of the proposed sensorless control during speed reversal.

It is evident from Figs. 6.a that the flux of the IM remains unaffected during the transient of the speed.

Some further tests are conducted next, to further verify decoupling of the control of the machine and the capability of the sensorless control scheme.

Figs. 7.a-7.c show the simulation results from stator flux control test. The speed references of IM is 50 rad/s. In Fig. 7.c the estimated flux tracks the reference perfectly.

Under the same condition the practical results are obtained which are shown in Figs. 8-10 respectively. It is seen that there is a good agreement between simulation and practical results.

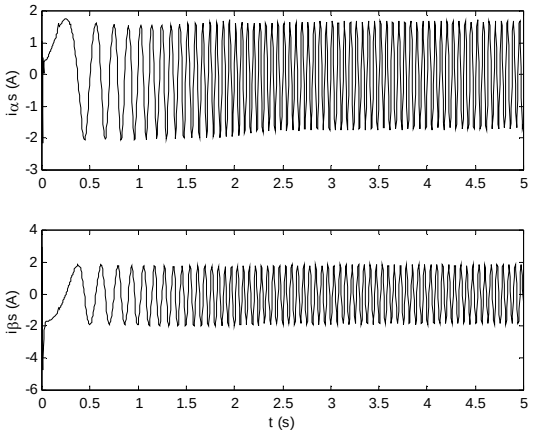

Fig. 5.c Simulation results: Stator current $\alpha - \beta$ components.

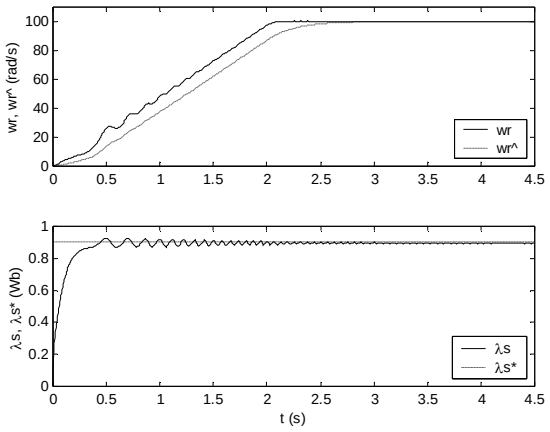

Fig. 5.a Simulation results: Speed and flux magnitude (speed start up test).

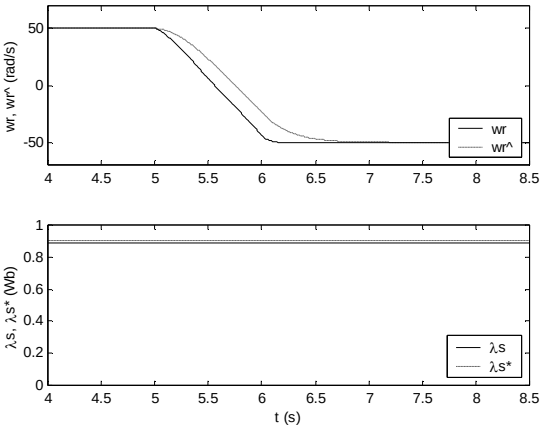

Fig. 6.a Simulation results: Speed and stator flux magnitude (speed reversal test).

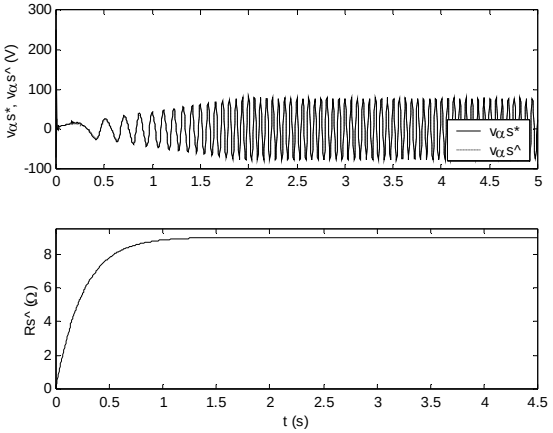

Fig. 5.b Simulation results: Stator voltage and estimated stator reference.

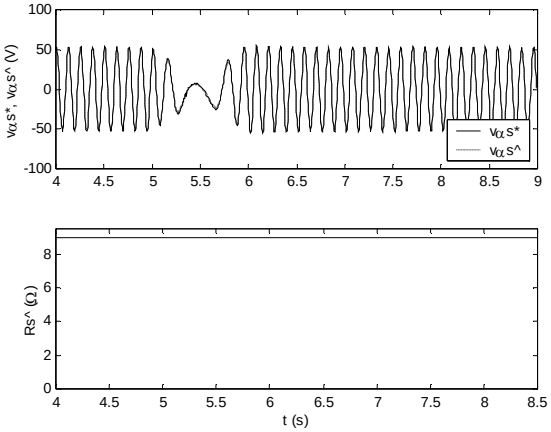

Fig. 6.b Simulation results: α component of stator voltage and estimated stator reference.

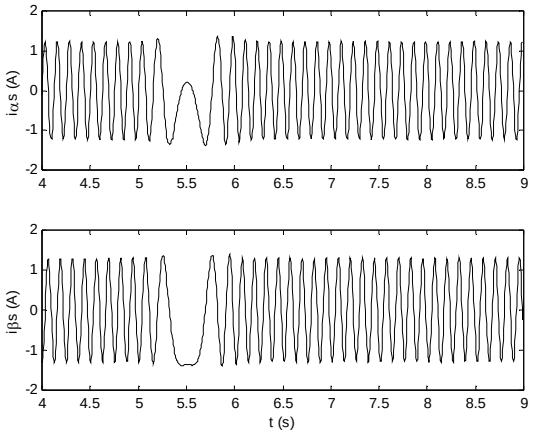

Fig. 6.c Simulation results: Stator current $\alpha - \beta$ components.

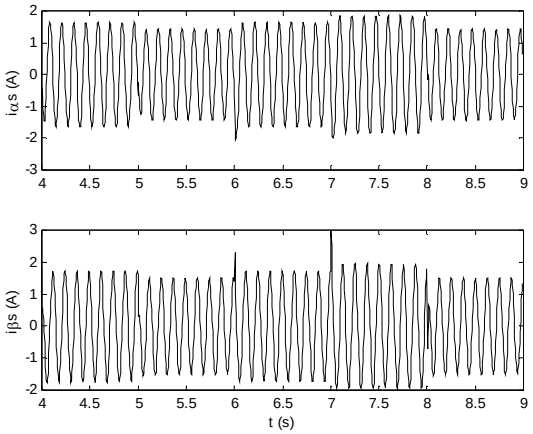

Fig. 7.c Simulation results: Stator current $\alpha - \beta$ components.

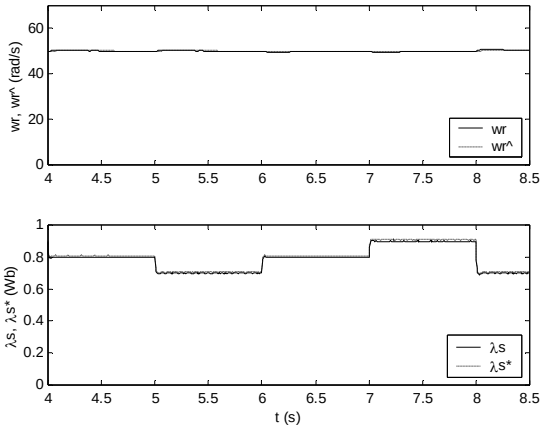

Fig. 7.a Simulation results: Speed and stator flux magnitude (speed start up test).

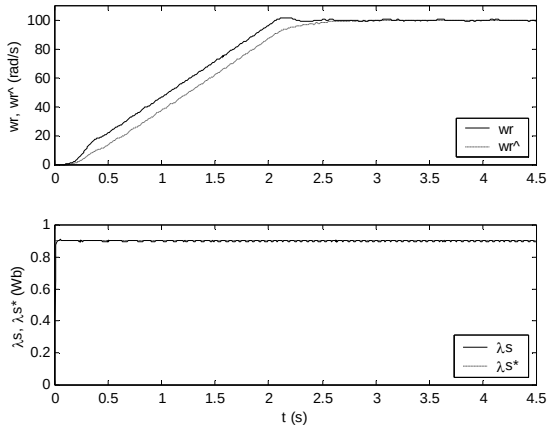

Fig. 8.a Experimental results: Speed and flux magnitude (speed start up test).

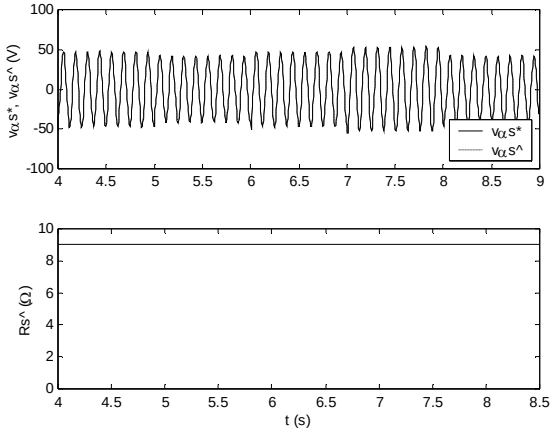

Fig. 7.b Simulation results: α component of stator voltage and estimated stator reference.

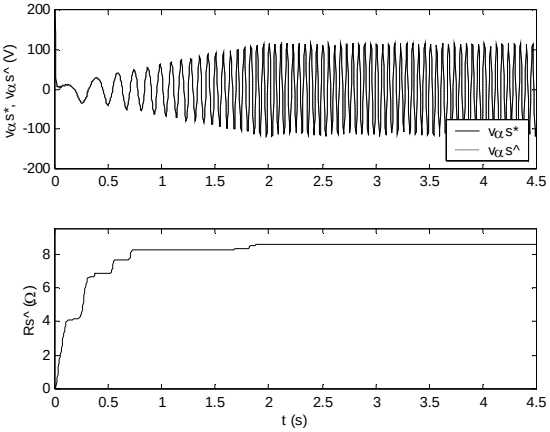

Fig. 8.b Experimental results: Stator voltage and estimated stator reference.

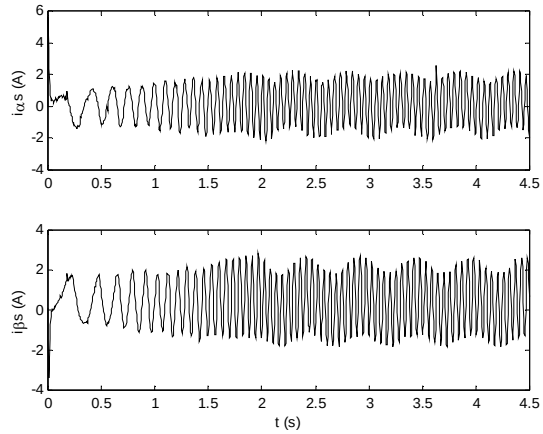

Fig. 8.c Experimental results: Stator current $\alpha - \beta$ components.

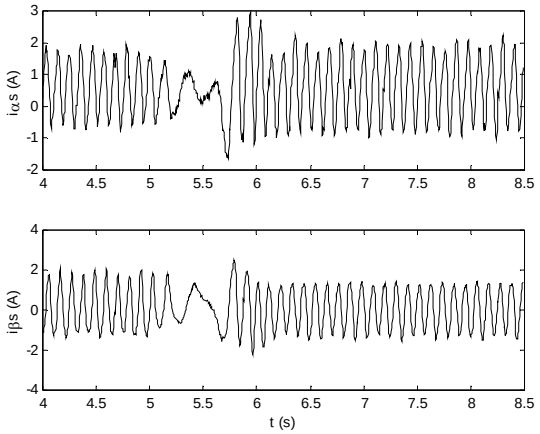

Fig. 9.c Experimental results: Stator current $\alpha - \beta$ components.

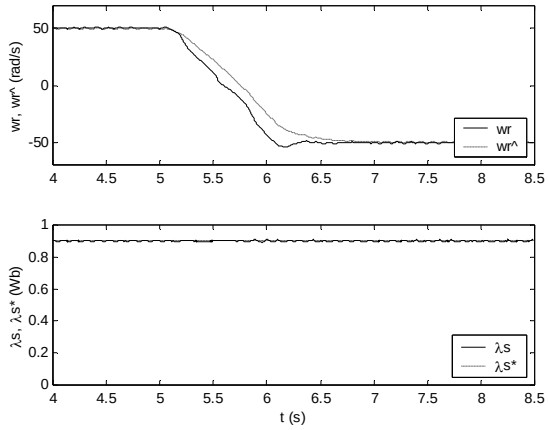

Fig. 9.a Experimental results: Speed and stator flux magnitude (speed reversal test).

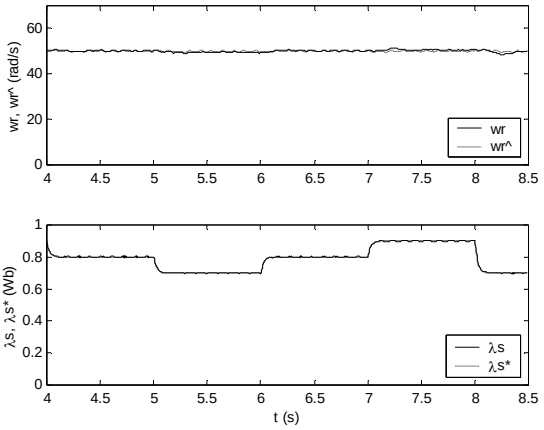

Fig. 10.a Experimental results: Speed and stator flux magnitude (speed start up test).

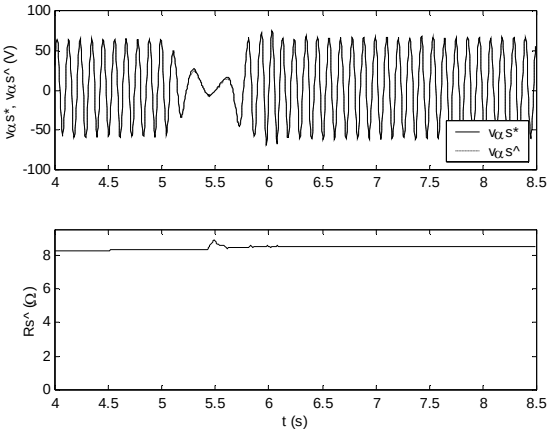

Fig. 9.b Experimental results: α component of stator voltage and estimated stator reference.

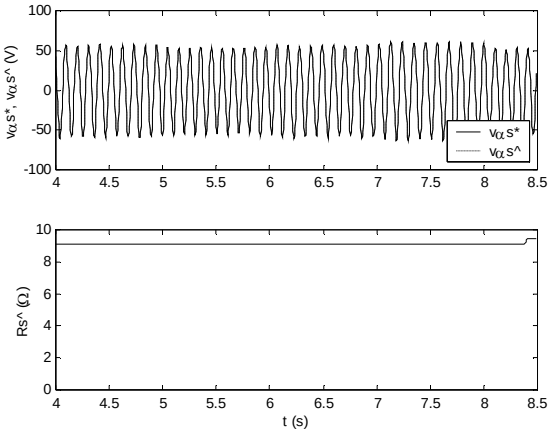

Fig. 10.b Experimental results: α component of stator voltage and estimated stator reference.

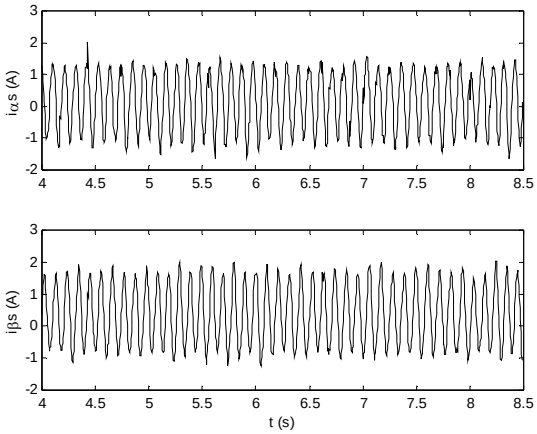

Fig. 10.c Experimental results: Stator current $\alpha - \beta$ components.

VII. Conclusion

A DTC-SVM scheme has been presented for an unsymmetrical six-phase IM. The decoupled torque and stator flux is achieved in the IM stator flux field orientation reference frame using conventional PI regulators.

In this control scheme, the rotor speed and stator resistance are estimated by simple estimation methods. In addition, the stator phase voltages are estimated by using the SVPWM inverter switching times and the dc link voltage.

Some simulation and experimental results has been presented to support the capability of the proposed control scheme. These two results are in a close agreement.

References

[1] E. Levi, S. N. Vukosavic and M. Jones, "Vector control schemes for series-connected six-phase two-motor drive systems", *IEE Proc.-Electr. Power Appl.*, Vol. 152, No. 2, March 2005.

[2] M. Jones, S. N. Vukosavic, E. Levi and A. Iqbal, "A Six-Phase Series-Connected Two-Motor Drive With Decoupled Dynamic Control", *IEEE Trans. on Ind. A*ppl., Vol. 41, No. 4, July/August 2005.

[3] R. H. Nelson and P. C. Krause, "Induction machine analysis for arbitrary displacement between multiple winding sets," *IEEE Trans. Power App. Syst.*, vol. PAS-93, no. 3, pp. 841–848, may/Jun. 1974.

[4] Y. Zhao and T. A. Lipo, "Space Vector PWM Control of Dual Three-phase Induction Machine Using Vector Space Decomposition", *IEEE Trans. on Ind. A*ppl., Vol. 31, No. 5, Sep./Oct. 1995, pp. 1100-1109.

[5] R. Bojoi, M. Lazzari, F. Profumo and A. Tenconi, "Digital field oriented control for dual three-phase induction motor drives," in *Proc. IEEE-IAS Annu. Meeting*, Pittsburgh, PA, 2002, CD-ROM, Paper 22P1.

[6] R. Bojoi, M. Lazzari, F. Profumo and A. Tenconi, "Digital Field-Oriented Control for Dual Three-Phase Induction Motor Drives", *IEEE Trans. On INDUSTRY Appl.*, Vol. 39, No. 3, May/June 2003, pp. 752-760.

[7] R. Krishnan and F.C. Doran, "Study of Parameter Sensitivity in High Performance Invereter-Fed Induction Motor Drive System". IEEE Trans. Ind. Application, vol. 23, no. 4, 1987, pp. 623-635.

[8] Radu Bojoi, Member, IEEE, Paolo Guglielmi, Member, IEEE, and Gian-Mario Pellegrino, "Sensorless Direct Field-Oriented Control of Three-Phase Induction Motor Drives for Low-Cost Applications", IEEE Trans. on Ind. Appl., Vol. 44, No. 2, March/April 2008, pp. 475-481.

[9] H. Jun, B. R. Duggal, M. Vilathgamuwa, "A MRAS-based speed sensorless field oriented control of induction motor with on-line stator resistance tuning", International Conference on Power Electronics and Energy Systems for Industrial Growth, Perth, Australia, December 1998, Vol.1, pp. 38-43.

[10] M. Ghanes, J. De Leon, A. Glumineau, "Cascade and high-gain observers comparison for sensorless closed-loop induction motor control", IET Control Theory Appl., 2008, Vol. 2, No. 2, pp. 133–150.

[11] M. Arkan, "Sensorless speed estimation in induction motor drives by using the space vector angular fluctuation signal", IET Electr. Power Appl., 2008, Vol. 2, No. 2, pp. 113–120.

[12] Koichiro Nagata, Toshiaki Okuyama, Haruo Nemoto, and Toshio Katayama, "A Simple Robust Voltage Control of High Power Sensorless Induction Motor Drives With High Start Torque Demand", IEEE Trans. on Ind. Appl., Vol. 44, No. 2, March/April 2008, pp. 604-611.

[13] Dramane Traoré, Franck Plestan, Alain Glumineau, and Jesus de Leon, "Sensorless Induction Motor: High-Order Sliding-Mode Controller and Adaptive Interconnected Observer", IEEE Trans. on Ind. Electr., Vol. 55, No. 11, Nov. 2008, pp. 3818-3827.

[14] Hassan K. Khalil, Elias G. Strangas, and Sinisa Jurkovic, "Speed Observer and Reduced Nonlinear Model for Sensorless Control of Induction Motors", IEEE Trans. on Control Systems Tech., Vol. 17, No. 2, March 2009, pp. 327-339.

[15] S. Doki, Y. Kinpara, S. Okuma, "Unified interpretation of indirect and direct vector control", PCC-Yokohama '93, 1993, pp. 297-302.